5 Cryostat

This chapter discusses the cryostat of the LZ detector. In particular it describes: the results of an extensive screening campaign and the simulations of associated backgrounds that lead to the cryostat material choice, cryostat technical specifications, design with key features, fabrication and tests requirements, and finally transportation and installation underground at SURF.

The cryostat will be fabricated by a specializing in titanium U-stamped pressure vessel manufacturer selected in the European Union tender process. The fabricator will be in charge of the supplied raw material processing including rolling and forging, cryostat manufacture, tests and certifications, cleaning, packaging and transportation to SURF.

5.1 Material Search Campaign

The LZ cryostat is one of the major contributors to the experiments background budget due to the mass of material required and the vicinity to the LXe target. This imposes stringent radiopurity requirements on its materials, and essentially limits the choices to copper, stainless steel and titanium although copper is rejected due to mechanical considerations. Titanium (Ti) has a high strength-to-weight ratio, low density and atomic number, and was previously sourced with low radioactivity by LUX [1]. The level of this radioactivity content would meet LZ requirements and the lower particle stopping power combined with considerably lower ^{60}Co content make it advantageous over stainless steel. The material studies and searches have therefore been focused on titanium. As a mitigation strategy against failing to source the material with adequate radiopurity and in sufficient quantity, on a sensible timescale, parallel studies have been conducted of stainless steel activity and a full cryostat design in that material has been developed.

Neutron and gamma-ray radioactivity from the cryostat is due to largely to uranium and thorium content in the construction material, as well as ^{40}K and ^{60}Co. To assess the typical concentration of these isotopes in titanium and stainless steel the complementary techniques of direct gamma-ray spectroscopy and and mass-spectrometry were employed. Samples were procured from various stages of production to inform typical activity, reproducibility of particular suppliers and points of inclusion of contamination - particularly for titanium.

5.1.1 Titanium

The production of Ti metal is a complex procedure that involves a number of stages in which additives and inclusions are deliberately introduced. Several such points in the production cycle may contribute to contamination of the final product with elements containing high concentration of radioactive isotopes such as ^{238}U, ^{232}Th, ^{40}K and ^{60}Co which are of particular concern. The refinement of the mineral concentrates, particularly for ilmenite, involves the addition of or exposure to coke, coal, oil, and tar prior to the chlorination process. It is not uncommon for such materials to contain relatively high levels of U and Th. However, the $TiCl_4$ produced at this stage undergoes chemical treatment and filtering to remove chlorides and sludge before pure liquid $TiCl_4$ is created, carrying away most impurities, including U and Th. Ultra-pure $TiCl_4$ is commercially available, as are titanium hydride and titanium nitride powders that are produced through plasmochemical processing from the $TiCl_4$. Beyond this stage, lack of sufficient contact controls with surfaces during the Kroll process and metallothermy present other potential sources of U and Th. However, the elements introduced, largely Mg and Ar, will probably not be problematic. The Ti sponge post-Kroll processing is exposed to several stages in which U and Th can enter the chain. Ti ingots and slabs are produced by pressing and melting the Ti sponge, yet often Ti alloy and Ti scrap is added at this stage. Other alloys such as aluminum and vanadium may also be included. Radioactive contamination contained within the scrap and alloys is then carried through to the Ti ingot and into the roll stock. The major stages of this production process, indicating inclusion points, are depicted in Figure 5.1.1 [2].

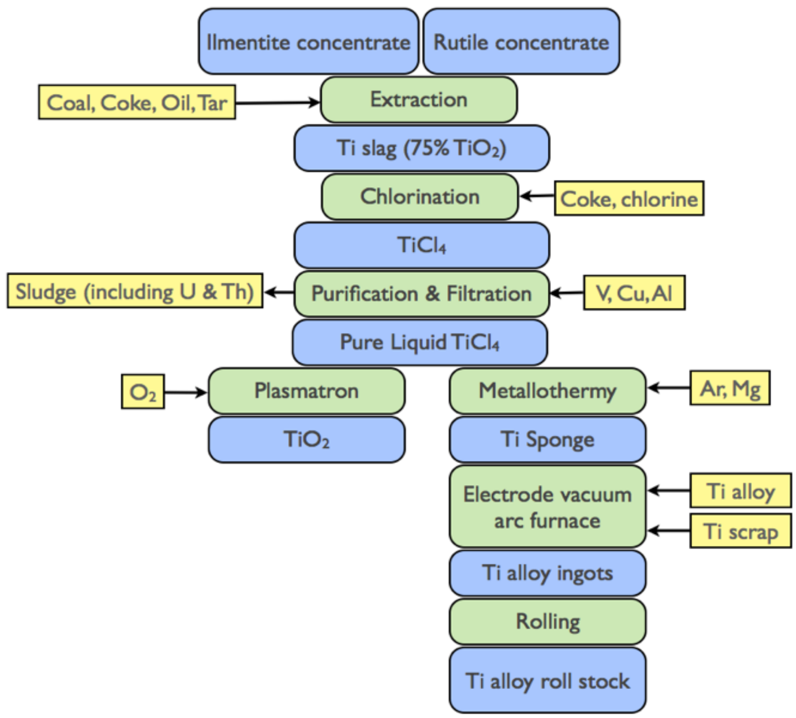

Figure 5.1.1: The commercial production of Ti metal, indicating the major stages (green boxes), the post- processing products (blue boxes), and the additives, as well as reductions during the procedure (yellow boxes). Figure adapted from [2]

In the material search campaign we have engaged several titanium providers including VSMPO [3], TIMET [4], Supra Alloy [5], Honeywell [6] and PTG [7] to provide sample material, taken from various stages along the production process, in order to determine where radioactivity, particularly U and Th, enters the chain. In our campaign we have received 23 samples including: eight sponges (TIMET), one sample of very high purity Ti (Honeywell), one Gr-1 with 10% scrap (VSMPO), two Gr-2 sheets (Supra Alloy and PTG), seven Gr-1 sheets (Supra Alloy, PTG and TIMET) and also Ti bolts and nuts. Table 5.1.1 summarizes all the Ti samples that have been radio-assayed in this campaign. Upper screening limits are indicated in italics.

5.1.2 Stainless Steel

Low background experiments searching for dark matter or neutrino-less double beta decay, such as XENON 1T [8] and PANDA-X [9], or GERDA [10] and NEXT [11], respectively, use stainless steel for their cryostats, with the majority of materials coming from German stockholder NIRONIT [12]. 13 samples were procured from NIRONIT for radio-assay. Independent assays of samples received directly from the GERDA and NEXT experiments were conducted to cross-check published results [13, 14] and to measure radioisotopes

Table 5.1.1: Summary of the 22 titanium samples assayed for LZ cryostat, including various grades and types from multiple suppliers.

#	Supplier	Sample name	^{238}U [mBq/kg]		^{232}Th [mBq/kg]		^{40}K [mBq/kg]	Titanium
			early	late	early	late		grade/type
1	Supra Alloy	Carlson 8J10	31.00	4.10	0	2.80	*1.80*	Gr-1 Sheet
2	TIMET	Osaka 26-29461	*2.50*	248	0	*4.10*	*12.0*	Sponge
3	TIMET	Tanghsan TX027594	*2.50*	6200	0	*2.50*	*15.0*	Sponge
4	TIMET	Toho C 12009C	*2.50*	*62*	0	*1.60*	*12.10*	Sponge
5	TIMET	Toho W 112266W	*2.50*	124	0	*1.60*	*12.00*	Sponge
6	TIMET	Zaporozhye 6680-12	*2.50*	744	0	*1.60*	*12.00*	Sponge
7	TIMET	Zuny TX027641	*25.00*	2480	0	4.1	*12.00*	Sponge
8	TIMET	HN0021-B/1	11.00	*0.60*	0	*0.60*	*2.50*	Gr-1 Sheet
9	TIMET	HN0021-B/2	4.90	3.33	2.85	0.80	*1.50*	Gr-1 Sheet
10	PTG	ATI W74M	46.00	2.80	0	2.80	*1.80*	Gr-1 Sheet
11	Supra Alloy	Timet BN3672(2) RMI 404666 (9)	110.00	*2.40*	0	170.00	2.40	Gr-2
12	PTG	Thyssen Krupp 611292	*9.60*	3.60	0	2.40	*2.10*	Gr-2
13	TIMET	Henderson 22-49312	*3.70*	2480	0	12.30	*18.00*	Sponge
14	S6MB annulus	Bolts	13000.00	*6.00*	0	160.00	*60.00*	Bolts
15	EE-33 full	Nuts	500.00	*8.40*	0	80.00	*60.00*	Nuts
16	Honeywell	T149858991	3.70	4.69	0	1.63	*1.50*	Gr-1 Sheet
17	VSMPO	528 g	*61.70*	*6.20*	0	*4.10*	*31.00*	Gr-1 Metal 10% scrap
18	VSMPO	996 g	17.28	12.35	0	*4.10*	*6.20*	Gr-1 Sponge
19	TIMET	HN2470	8.51	0.37	0	0.61	0.52	Gr-1 Sheet
20	TIMET	Master ID #46	8.00	*0.124*	0	*0.12*	*0.62*	Gr-1 Sheet
21	TIMET	HN3469-T	*1.6*	*0.1*	0.31	0.30	*0.62*	Gr-1 Slab
22	TIMET	HN3469-M	2.90	*0.10*	*0.2*	0.25	*0.68*	Gr-1 Slab

not reported, as well as early U and Th activity. The 13 samples (a total of 152 kg) originated from different heats and were made by different mills: 7 samples at Thyssen Krupp Nirosta (Germany) and 6 samples at Aperam (Belgium). All samples were electro-polished at LBNL and pre-screened with a surface HPGe counter (MERLIN), particularly for excessive ^{60}Co. Samples with <20 mBq/kg of ^{60}Co were forwarded for more sensitive tests underground at SURF and at the University of Alabama. Stainless steel radio-assays are summarized in Table 5.1.2.

Table 5.1.2: Summary of the 13 stainless steel samples radio-assayed for LZ. Due to a high ^{60}Co content detected in samples 10 to 13 during pre-screening, these were not assayed further and as such early-chain contents were not measured

#	Sample name	^{238}U [mBq/kg]		^{232}Th [mBq/kg]		^{60}Co	^{40}K
		early	late	early	late		
1	NIRONIT 311113	7.3	0.35	1.1	4	14.5	*0.53*
2	NIRONIT 511803	1.2	0.27	0.33	0.49	1.6	*0.4*
3	NIRONIT 512006	*1*	0.54	0.49	1.1	1.7	*0.59*
4	NIRONIT 512844	1.4	0.5	0.5	0.32	2.6	*0.5*
5	NIRONIT 521663	1.9	0.38	0.81	0.73	5.6	*0.46*
6	NIRONIT 521994	0.5	1.9	1.7	1.5	4.5	*0.5*
7	NIRONIT 124113	0	1.1	0	4.1	8.2	*3.0*
	NIRONIT (Alab) 124113	0±22	4.89	0	5.37	14.6	1.7
8	NIRONIT 211093	0	*0.6*	0	*0.8*	7.4	*3*
	NIRONIT (Alab) 211093	0±11	2.46	0.0	0.37	14.0	0
9	NIRONIT 528292	0	*0.6*	0.0	*0.9*	6.5	*3*
	NIRONIT (Alab) 528292	0±22	2.22	0	0.67	9.69	0
10	NIRONIT 832090	0	4	0	2.2	26	*4*
11	NIRONIT 407156	0	*0.6*	0	4.8	32	*2*
12	NIRONIT 528194	0	*0.8*	0	2.1	32	5
13	NIRONIT 828660	0	*1.4*	0	*1.5*	335	*4*

After screening 23 Ti and 13 Stainless Steel samples in the material search campaign for the LZ cryostat, we have concluded that the highest and reproducible radiopurity is achieved with Commercially Pure Grade-1, as per ASTM B256, Ti without added scrap material and using Cold Hearth Electron Beam (CHEB) refining technology. CHEB used for production of commercially pure Ti provides an important purification mechanism in which high density contaminants are removed by gravity separation. By contrast Vacuum Remelting Technology (VAR) does not have such material refining capabilities. All samples of the finished material supplied by TIMET were produced with such recipe. Their radioactivity levels were consistent and always below the LZ acceptance criteria. Samples HN3469-T and M were from a 15,000 kg Ti jumbo slab that TIMET produced at its mill in Morgantown (Pennsylvania) and made available for the LZ cryostat. We note that the screening results of those samples represent the lowest radio-impurity contamination ever reported for a titanium sample.

5.2 Monte Carlo simulations of background from the cryostat

Radioactive background due to the cryostat vessels has been evaluated by means of the detailed Monte Carlo simulations as described in 12.1, which is an evolution of the simulation developed for the LUX [15], based on the GEANT4 simulation toolkit [16]. Whilst sharing the same physics models and software structure, the package developed for LZ has been implemented with the detailed geometry of the LZ detector including shielding, cryostat (inner and outer vessels, flanges and bolts), inner detector, photomultiplier tubes (PMTs), PTFE reflectors, the cathode and anode grids, field shaping rings, and outer detectors comprising the LXe skin, and the Gd-doped liquid scintillator. The outer detectors are implemented appropriately as veto systems in these simulations.

For neutrons, (α,n) reactions and spontaneous fission neutron energy spectra were generated using the SOURCE software [17]. These spectra were then embedded into the simulation framework, which propagates neutrons isotropically emitted from the cryostat. Only neutrons from (α,n) reactions contribute to the nuclear recoil (NR) events background, thanks to the the very high efficiency of the LZ detector in vetoing neutrons from the spontaneous fission process, as described in Section 12.1.2.1. We evaluate separately the early and late part of the ^{238}U enabling us to properly consider samples in which the secular equilibrium is broken.

For electron recoil (ER) events from ^{238}U and ^{232}Th decay chains, and ^{40}K and ^{60}Co, we used a new particle generator, described in Section 12.1.2.3, based on the standard GEANT4 process.

To achieve the required sensitivity of 3×10^{-48} cm^2, we set as a goal the total ER event rate from detector materials to be below 10% of the rate from pp solar neutrinos in the WIMP search region, 1.5 keV$_{ee}$ to 6.5 keV$_{ee}$, and the NR event counts to be below 0.2 events after S2/S1 discrimination in the full run time of 1,000 days, within 6 keV$_{nr}$ to 30 keV$_{nr}$.

The impact of the cryostat on the background counts has been estimated by the full detector and physics simulation, and is presented in Figure 9.2.1. The plot shows the results for Ti (TIMET) and stainless steel (NIRONIT) samples for LZ in the 1,000 d exposure with a 5.6 tonne LXe fiducial volume and after all the veto systems are applied, for ER events within 1.5 keV$_{ee}$ to 6.5 keV$_{ee}$, with 99.5 % rejection, and within (6–30) keV$_{nr}$, and 50 % acceptance, for NR events. The Ti identified by the assay program, indicated by the star corresponding to 0.53 counts for ER and 0.01 counts for NR, is well below the requirements for LZ, for a specific detector component.

5.3 Cryostat technical specification

The intended purpose of the cryostat is to hold 10,000 kg of liquid xenon at −100 °C with an immersed Time Projection Chamber in it. The cryostat consists of three main sub-assemblies: an Inner Cryostat Vessel (ICV), an Outer Cryostat Vessel (OCV) separated by a vacuum space and a Cryostat Support (CS). The cryostat is submerged in a water tank and surrounded by the outer detector acrylic vessels filled with a liquid scintillator. A general view of the cryostat with the acrylic vessels below (supported by the CS shelves) and above (supported by the OCV head and flange) is shown in Figure 5.3.1.

The material for the LZ cryostat is commercially pure Ti, Grade 1 per ASME SB-265, with additional low-radioactivity background requirements as presented in 5.1. The design of the vessels complies with the following codes: ASME BPVC [18], 2012 Int. Building Code, and ASCE 7 [19], with site soil classification Class B (Rock) for seismic conditions. The 2008 U.S. Geological Survey hazard data for this location are: S_S = 0.121 g, S_{MS} = 0.121 g, and S_{DS} = 0.081 g. The Seismic Design Force for LZ is 0.054 g, which imposes a force of 6350 N at the center of mass of the cryostat during a seismic event. The LZ cryostat operational temperatures (°C) and pressures (bar absolute) are summarized in Table 5.3.1

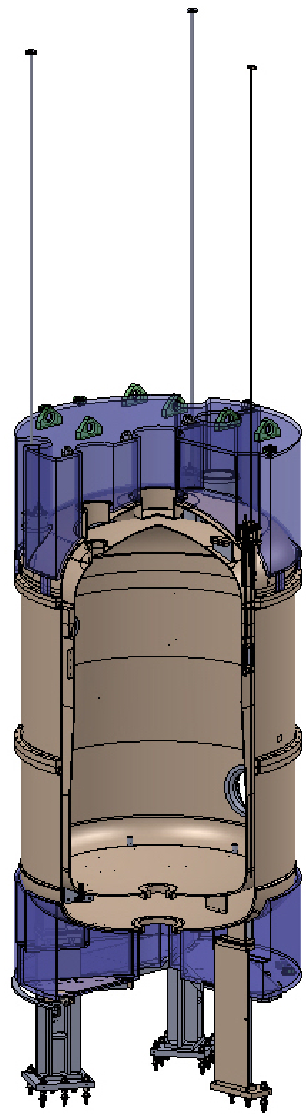

Figure 5.3.1: LZ cryostat assembly with the ICV nested in the OCV supported by the three legs of the CS. Acrylic vessels of the Outer Detector are shown at the top and bottom of the OCV. Three equally spaced vertical tubes will be used to deliver calibration sources into the vacuum space between the vessels.

Table 5.3.1: Pressures and temperatures for cryostat operational conditions: normal, bake out and most severe failures.

Vessel	Pressure [bar absolute]		Temperature [°C]	Condition
	Internal	External		
Inner	≤4.0	Vacuum	−112 to 37	Normal
	Vacuum	1.01	≤100	Bake out dry, no water in water tank
	Vacuum	1.48	−112 to 37	Failure mode water flooded between inner and outer vessels
Outer	Vacuum	1.48	0 to 37	Normal
	Vacuum	1.01	≤100	Bake out dry, no water in water tank
	1.48	1.01	0 to 37	Failure mode Xe gas leak between inner and outer vessels and no water in water tank

5.4 Inner Cryostat Vessel

The ICV has conventional cylindrical geometry with ellipsoidal heads, as shown in Figure 5.4.1. The inner vessel is split once near the top head with a flange pair. To minimize the passive volume filled with LXe, the diameter of the inner vessel is tapered near its half-height and the bottom head has an ellipsoidal shape with a 3:1 aspect ratio (the top head has the more common 2:1 aspect ratio). The 3:1 aspect ratio head requires greater material thickness compared to the 2:1 head, but this trade-off is well worth the savings in LXe.

For internal pressure, the thickness of the vessel walls in the cylindrical section is governed by a straightforward formula in the pressure vessel code. The minimum wall thickness is a function of the material, vessel diameter, pressure, and quality control measures. At the required internal pressure, the minimum wall thicknesses in the cylindrical section is 5.5 mm. A number of ports are necessary to carry fluids and electrical signals to and from the inner detector. These are added to the top and bottom heads, as well as a side penetration for cathode high voltage. The latter is discussed further in Sections 3.3. Buckling is an important failure mode to consider for vessels that see external pressure (vacuum in this case). The ASME BPVC specifies safe external working pressures based on material, temperature, wall thickness, diameter, and length. If the allowable external pressure is insufficient, a vessel designer has a couple of options. The first is to increase the wall thickness. In the case of LZ, this is undesirable for a number of reasons: Most notably, it creates more background radiation and reduces veto efficiency. The other option is to add reinforcing rings. Reinforcing rings essentially shorten the length of the vessel from a buckling perspective. To comply with the ASME code, a stiffening ring is located at the top of the tapered (conical) section of the inner vessel. This ring acts as a line of support to increase buckling resistance, and therefore allows a thinner wall to be used, e.g. 6 mm instead of 8 mm. Comparing the values for internal pressure 4 bar versus external pressure 1.48 bar, it is evident that the vessel design is driven by external pressure. It should also be noted that the minimum wall thickness is the minimum as-built, not the nominal. During the head-forming process, for instance, flat material is drawn or spun into shape, and in that process thinned from its original

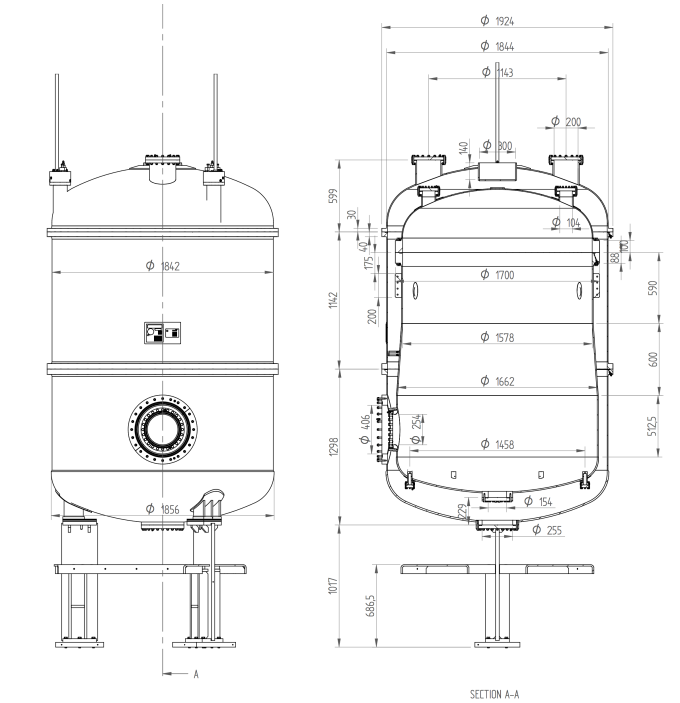

Figure 5.4.1: LZ cryostat assembly. Dimensions of major components are shown.

thickness. It should also be remembered that material is commercially available in discrete increments as opposed to infinitely variable thickness. Total mass and minimum thicknesses required by the ASME code for each segment of the inner and outer vessel made of Ti are summarized in Table 5.4.1.

Table 5.4.1: Vessel-wall thicknesses [mm] and total mass [kg] imposed by the external pressure at the normal, bakeout and failure conditions.

Inner Vessel						Outer Vessel			
Top head	Upper wall	Conical section	Lower wall	Dished end	Total mass	Top head	Side wall	Dished end	Total mass
7	9	9	9	11	950	8	7	14	1115

To minimize the amount of LXe between the TPC and the inner cryostat, the shape of the inner vessel is tapered at its half-height. Studies of the electric-field distribution show that the electric field is below the maximum allowed value of 50 kV/cm. The inner vessel will be sealed with a sprung metal C-seal because at the experimental temperature, O-ring seals with typical elastomeric materials are not suitable. Additionally, the large diameter prohibits the use of a knife-edge flange. Smaller ports on the vessels will be sealed with sprung metal C-seals as well. Inner-vessel flanges with C-seal gaskets for cryogenic service will also feature a secondary O-ring seal to facilitate room-temperature leak detection.

5.5 Outer Cryostat Vessel

The OCV supports the ICV through three tie bar assemblies situated in the top head. The ICV contains the TPC and LXe. The ICV can be leveled by adjustment of the tie bars externally from above the water tank.

The OCV also provides support for top and bottom Liquid Scintillator tanks, access to the vacuum space for calibration purposes and ports in the top head for cryogenic and cable services. At the bottom a LXe recirculating system of pipes connects to the lower port. The OCV base interfaces with the CS and its position in the water tank determines the orientation of the HV port in the base of the vessel. The HV ports of both vessels are aligned for the umbilical connection.

The OCV, as shown in Figure 5.4.1, has been designed in three pieces for ease of transport to the Davis cavern and assembly in the water tank it is joined together around the circumference by two flange pairs. The top head comprises a flange, 2:1 ellipsoidal head, three ports for the ICV suspension, two conduit ports for cryogenic and cabling services and a large central recess for a calibration source called “YBe”. The middle section of the OCV is a straight cylinder with two flanges that match the head and base flanges. The flanges are double-sealed with two elastomer O-rings and a pump path between the two to facilitate leak detection. Both O-rings are expected to seal at experimental temperatures since the OCV operates close to room temperature. The bottom head comprises a flange that matches the middle section, a HV port that enables the umbilical to be connected to the vessel, three support feet welded to the 2:1 ellipsoidal head and a heat exchange port flange centrally situated in the head. Each foot has a 6.3 mm diameter survey hole in the 20 mm-thick plate at the outer surface. The flanges are joined with stainless steel bolts and nuts (M12, 48) (same grade as for the ICV and supplied by the LZ project). All flanges must be integral design. To facilitate assembly, tapered pins have been incorporated into the design. During assembly and leak testing, the conduit ports, tie bar ports, HV and HX ports will be sealed with blanking plates. The sealing plate for the tie bar ports on the OCV head has the feature of a hoist ring to lift the head or vessel assembly. The tie bar assemblies themselves are used for lowering the ICV into the OCV during final assembly.

The ICV is suspended from three tie bar assemblies situated in the OCV head. Cross section of the tie bar is shown in Figure 5.5.1. They incorporate an adjustment feature for leveling the ICV and the tie bar is sealed into the assembly with a metal bellows that facilitates vertical movement with a small angular offset.

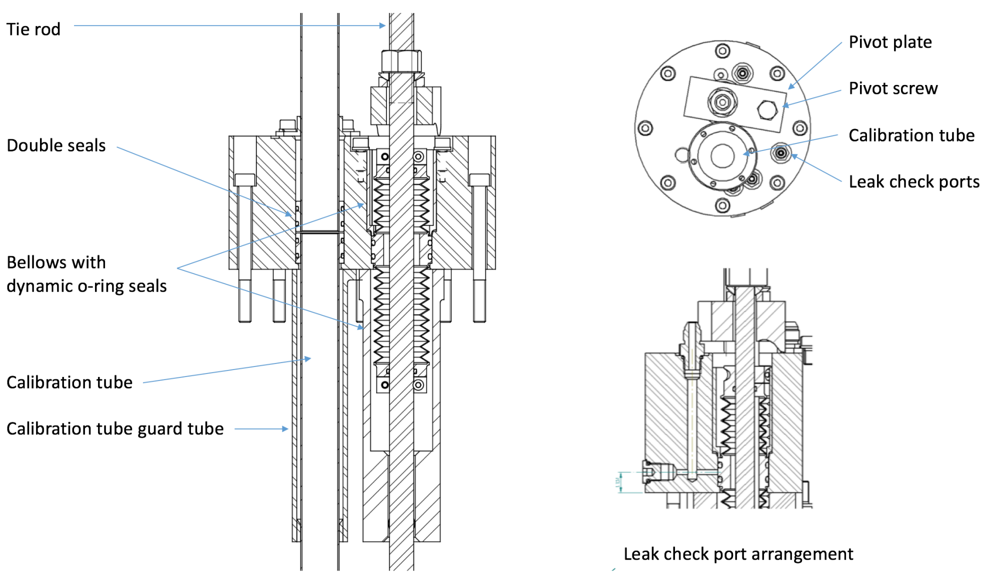

Figure 5.5.1: OCV tie rod port assembly

There is a coarse and fine adjustment the fine adjustment uses a pivot plate giving a 3:1 advantage. Also housed within the assembly is a calibration tube that facilitates access to the vacuum space between the vessels and enables a calibration source to be lowered down to within a few mm of the ICV lower head. The inner diameter and the wall thickness of the tubes are 25.4 and 0.94 mm, respectively. The length of the tube spans from the deck above the cryostat to the tangent line of the OCV dished end.

Double seals are used throughout the LZ cryostat and the volume between the grooves is accessed with a sealed nipple that is used to detect leaks between seals. The tie bar assemblies have four of these items to access the seals. The tie bars are manufactured from high strength stainless steel giving a factor of safety of 3:1.

5.6 Cryostat Support

The CS structure has been designed to support the operating load and resist a horizontal force due to a seismic event. The CS interfaces with three base plates mounted on studs protruding from the water tank base these plates will be surveyed and adjusted flat and level at the correct height for the umbilical. Holes for survey targets have been included in the relevant faces of the legs for this purpose. The support has been designed with stability, strength and installation in mind. The cryostat interfaces with flange plates welded to the top of the legs and is shimmed to the correct height. The support has also been designed with the requirements of the veto counter in mind and maximum coverage by the LS tanks has been achieved with a three leg flat plate design. The three segmented tanks fit between the legs and are supported on shelves between the legs.

5.7 Cryostat Interfaces

The cryostat interfaces with many other subsystems of the experiment. Some of them are physically connected to its ports creating additional loads which must be considered in the cryostat design. External loads imposed by the other subsystems on the cryostat ports are listed in Table 5.7.1. In addition, the feet of the ICV and OCV shall withstand the load of the vessels when filled with water for the hydrostatic tests.

5.8 Thermal Insulation

It is important to limit the heat transfer between the inner vessel and the environment to minimize the amount of refrigeration needed underground. In addition, reducing heat transfer helps to prevent unwanted convection currents in the LXe fluid. The vacuum between nested inner and outer vessels essentially eliminates thermal conduction and convection, in typical Dewar fashion. The dominant mode of heat transfer is therefore radiation, and with a large surface area ($\sim 16\,\mathrm{m}^2$) and a large temperature difference, it is potentially substantial. Multilayer insulation (MLI or superinsulation) is proposed as the baseline solution to reduce this thermal load during normal operation. MLI is a well-known insulating material for in-vacuum cryogenic service. The thermal load with and without this material varies by approximately an order of magnitude. In this case, the expected heat load with bare vessels would be several hundred watts, and with MLI several tens of watts. In LZ, the proposed amount of total refrigeration is about a kilowatt, so MLI is the clear choice. A 3-parts MLI blanket design for the ICV is shown in Figure 5.8.1.

MLI works well during normal operation, but is ineffective in the event of a failure in which a gross amount of liquid water enters the volume normally occupied by vacuum between the vessels. To mitigate this failure mode, a closed-cell polyurethane foam will be applied to the outer surface of the inner vessel anywhere it is in contact with LXe (basically everywhere below the main seal flange). The proposed foam thickness is 2 cm over the bottom head, and 1 cm over the remainder. MLI will be wrapped over the foam, and covers

Table 5.7.1: External loads to the cryostat in addition to any loads exerted by vessel internal and external pressures.*Combined load from cryostat, Outer Detector tanks and seismic load.**The moment due to the seismic load at 2/3 height.

Cryostat Item	Number of items	Maximum allowable load on a single item [N]	Maximum allowable moment in any direction to the flange face [Nm]
Inner Cryostat Vessel			
Top head port	2	200	200
Weir port	3	100	100
HV port	1	2000	2000
TPC port	6	3000	200
Dished end port	1	1000	1000
Outer Cryostat Vessel			
Top head port	2	1000	1000
YBe source port	1	3200	N/A
Top flange	2	10000	N/A
Tie bar port	3	33000	N/A
HV port	1	2000	1000
Bottom port	1	1000	1000
Cryostat Support			
Leg	3	50507*	15265**
Shelf	3 5000	N/A	

the entire inner vessel and its cold appendages. With the foam in place, the maximum heat transfer in this failure mode is expected to be 3,600 W, which corresponds to a Xe boil-off of 450 standard liters per minute (slpm). This rate is within the Xe-recovery capacity of the system.

A dedicated thermal analysis has been carried out in order to investigate possible distortions in the calibration tubes from asymmetric thermal gradients caused by thermal radiation from the inner face of the tube onto the cooler cryostat. The steady state thermal simulation was carried out in Ansys CFX [20], and consisted of basic tubular geometries representing the outer and the inner vessels, with a nitrogen filled calibration tube geometry located between the two vessels in a vacuum interspace. Thermal radiation was modeled between the warmer OCV (20 °C) and the cooler ICV (−100 °C). For our preferred MLI product, (Coolcat 2 NW) the supplier - Ruag [21] specify that 10 layers at 300 K to 77 K give heat loss of <1 W/m^2. Using the equation E_{eff} = P/S x (T_h^4 T_c^4) the average effective emissivity over this range is 0.002,2 W/mK. A more conservative emissivity value of 0.025 W/mK has been used for the simulation and this value was backed up by wider research of similar MLI products, and also by data used for the cryostat vessel heat transfer calculations. Based on these boundary conditions, the maximum thermal gradient over the length of the calibration tubes was found to be negligible, resulting in a maximum deflection at the end of the tube of less than 0.1 mm.

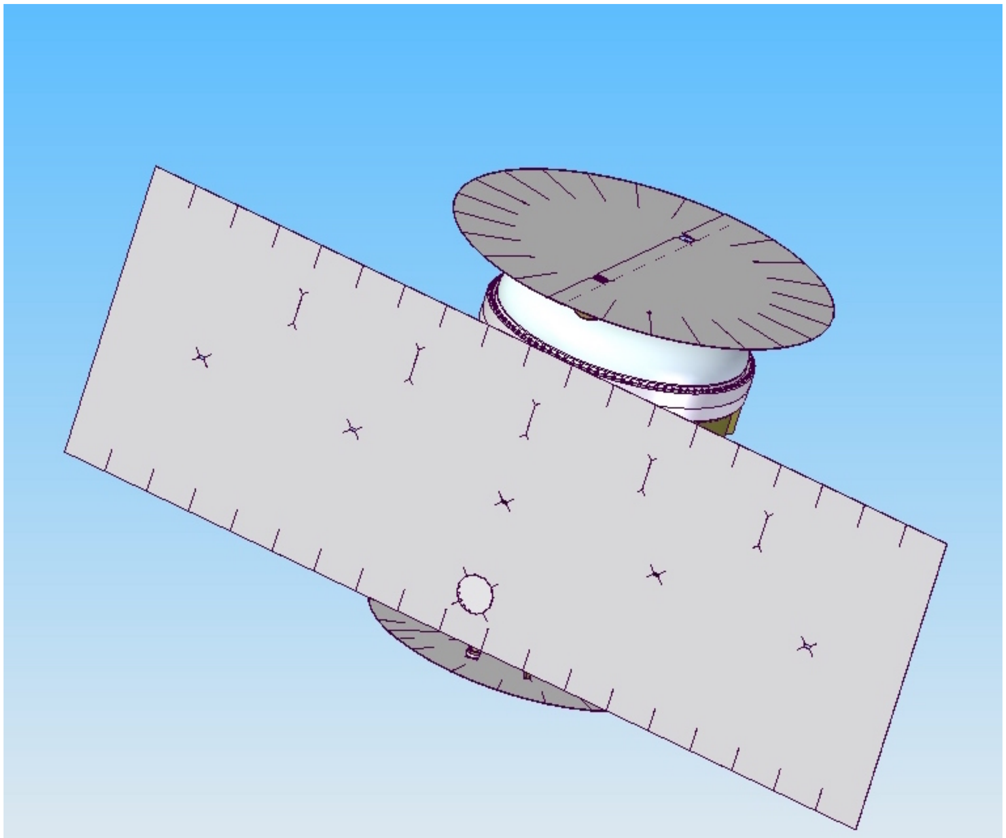

Figure 5.8.1: Three parts of the MLI blanket for the ICV thermal insulation.The design with only three parts has been chosen to effectively cover the whole ICV surface with a minimum work required for its assembly. Only final sewing will be needed. Several holes have been provisioned for ICV features such as: ports, fins, tie rods and seismic limiters. Cuts along the blanket's edges are to facilitate wrapping on curved surfaces of the vessel heads.

5.9 Fabrication, Cleanliness, Tests and Certifications

The titanium for the cryostat is extremely rare and difficult to obtain and as such contingency provision shall be made for spare material. Potential fabricators are required to demonstrate that they have built in an acceptable level of contingency and that they will take the necessary manufacturing precautions in order to minimize waste and ensure that they do no not exceed their allocation.

Together with the cryostat design, a comprehensive set of drawings has been made which contain toleranced geometric specifications. The general tolerance on machined parts of the cryostat such as flanges and mating surfaces is 1 mm. This tolerance has been relaxed on the form of the barrels in most cases, and wherever possible in order to aid the ease of manufacture. Where squareness, flatness, position of holes and other features are important for full assembly these are generally tightened to 0.5 mm. Several key features of the cryostat assembly are highlighted below:

- The ICV top head conduit ports must align with those in the OCV with a tolerance of 2 mm.
- The HV port in the ICV has a squareness tolerance of 1mm relative to top flange and can be positioned ±1 mm from that flange. There is also a ±1 mm tolerance applied to the face from the vessel wall. The

face has a positional tolerance of 0.8 mm from the tie rod holes. The required flatness is 0.5 mm and the positional tolerance of the tie rod holes is ±0.8 mm.

- The HV port in the OCV has a squareness tolerance of 1 mm relative to the flange in the base and a linear tolerance of ±1 mm to the flange tangent line. The required flatness is 0.5 mm. The tie rod ports in the OCV head have a positional tolerance of ±1 mm.
- For helicoflex seals, the manufacturers [22] specifications have been used, and for the O-ring grooves, BS1806 standard tolerances have been used.

Meeting the geometric requirements of form and alignment of key features can be particularly challenging when producing titanium weldments, where components are prone to distortion during machining and welding procedures. The cryostat shall be welded according to ASME IX BPVC [23]. GMAW or MIG welding should be used and the consumable electrode/welding rod shall be the same titanium material as the vessel raw material. Welding of titanium is a specialist process and the manufacturing contractor is required to demonstrate they are titanium welding specialists with particular emphasis on pre-weld preparation/cleaning, and on protection of the heat affected zone from oxidation during welding. They are required to outline their weld acceptance criteria such that it may be assessed by LZ.

A very high level of cleanliness is required for any component of the cryostat vessels throughout production. Every reasonable effort shall be made to minimize cross-contamination with swarf and loose dust of foreign material as well as environmental radon plate-out on the cryostat surfaces. The project goal is to achieve a dust level for the internal surface of the cleaned and packaged ICV of 10 ng/cm^2. For all other surfaces the dust level shall not exceed 1 μg/cm^2 at delivery. The following procedures shall be applied: the cryostat raw material shall be stored separately from other material in the workshop; parts shall be individually bagged in the bags provided by LZ to avoid any dust accumulation on the surfaces. Bagged components shall be placed on wooden pallets inside the pallet footprint, safe from the risk of impact or damage to the bag. The cleaning process for stock material at the mill shall follow the ASTM B 600 standard. Grease, oil and lubricants are to be removed with alkaline or emulsion type cleaners only. No mechanical abrasion type cleaning is allowed. A surface layer of at least 5 microns shall be removed from all stock material by pickling/etching with virgin chemicals. Chemicals shall be rinsed off after etching with deionized water. Prior to machining, rolling and spinning all surfaces in direct contact with cryostat components shall be cleared of dust and swarf with a stiff non-metallic brush, and cleaned with solvent using a lint-free cloth. All machines shall be flushed of coolant, and coolant replaced with fresh, water soluble coolant, approved by LZ. During machining, cryostat components shall be separated from other materials in the workshop, and the work area kept clean and tidy. Post manufacture, all components awaiting further processing shall be hand de-greased with solvent and a lint-free cloth before being bagged using bags provided by LZ, and stored in a clean place.

Prior to welding, components shall be comprehensively cleaned. Dirt, oil and dust shall be removed from the weld area, and oxide/scale removed by etching. All surface tables and tools in contact with any part of the cryostat shall be cleaned by hand with fresh solvents. Upon completion of welding, components shall be bagged using LZ provided bags and stored in a clean place. Heavy abrading, grinding or wire brushing is prohibited both before and after welding. For final cleaning, all faces of the cryostat vessels shall be etched using LZ approved virgin chemical solution, and in accordance with ASTM B 600 standard, removing at least 5 microns from all surfaces. Parts shall then be rinsed with deionized water and thoroughly dried. All parts shall then be bagged, purged with nitrogen and sealed.

With cooperation from the manufacturing contractor, LZ will carry out the following cleanliness and radioactivity testing: after etching of raw material, a representative 10 kg coupon shall be cut from the 8mm stock plate along with all off-cuts from vessel ports and reinforcement pads, and swarf from bolt holes in large flanges shall be retained and radio-assayed at SURF. In addition, 10 kg of Ti welding rods and 10 kg of sample welds shall be sent to SURF for radio-assay. The impact of etching on the dimensions of critical features such as grooves shall be assessed prior to machining the real grooves. LZ shall measure the levels of radon present at various fabrication and cleaning locations.

The following tests will be conducted by the manufacturing contractor and witnessed by designated persons from RAL/STFC:

- A dimensional check of all components of the cryostat as well as its assemblies, including a localization of the survey markers in 3D space relative to the key features.
- Provide proof by mechanical assembly and documentation that the sequence of assembly at SURF shown in Figure 5.10.1 is achievable.
- Test and record ICV and OCV leak rate demonstrate that the leak rate does not exceed 1×10^{-6} mbar l/s (helium).
- Conduct a pressure test ICV and OCV for the internal pressure case per the ASME BPVC, as required to achieve certification.
- Conduct a suspension full load/leak test of ICV with tie bars assembled. The ICV shall be loaded to 1.5 x 33,000N = 49,500N and the upper part external to the vessel shall be exposed to water at the operating pressure of 1.48 bar absolute. The lower part of the vessel shall be evacuated and vacuum leak rate measured and certified to be below 1×10^{-7} mbar l/s. Further details are contained in the cryostat specification document.
- The cryostat support shall be full load tested with 12T applied in increments of 4T, with lateral deflection of the legs as well as vertical displacement of the support recorded. Measured deflection for each leg shall be smaller than 1 mm.
- The vessel shall be stamped/marked relating to the testing and approval. This shall not impart dirt into the system or be etched away during cleaning.

5.10 Transportation and Installation

The cryostat inner vessel along with its contents will be moved as an assembly down the Yates shaft at SURF. The width of the shaft is nominally 1.85 m, and the maximum payload width is 1.70 m to clear features in the shaft cross section and provide some margin of safety. The outer vessel in contrast will be moved down the Yates shaft in three pieces, and assembled once in the Davis Cavern.

The CS will be placed onto three base plates that are independently supported inside the water tank. The plates will have been leveled and surveyed prior to the LZ installation. An assembly procedure will be carried out at the manufacturers which will as closely as possible reproduce what will be carried out in the tank at SURF. Having placed the CS onto the plates and loosely assembled the fixing bolts the base of the outer vessel will be assembled onto the top supporting flanges with bolts and shims in place. The shelves between the legs for supporting the LS tanks must be included in this assembly procedure. A preliminary inspection will be carried out to check that there are no gaps between the mating interfaces greater than 0.5mm. Any gaps greater than 0.5 mm will be shimmed with appropriate thicknesses of shim stock. When this has been completed and a dimensional check has established that the CS support and base are in the correct position the fixing bolts will be tightened sequentially to ensure the geometry is preserved. A trial assembly can now proceed following the sequence shown in Figure 5.10.1. Care must be taken at all times to protect sealing surfaces, the seals will will not be in place when this procedure is carried out at the manufacturer. The middle section of the outer vessel is assembled next onto the base flange using the assembly dowels to locate it in the correct orientation at this stage a minimum of six bolts can be used to hold the assembly together.

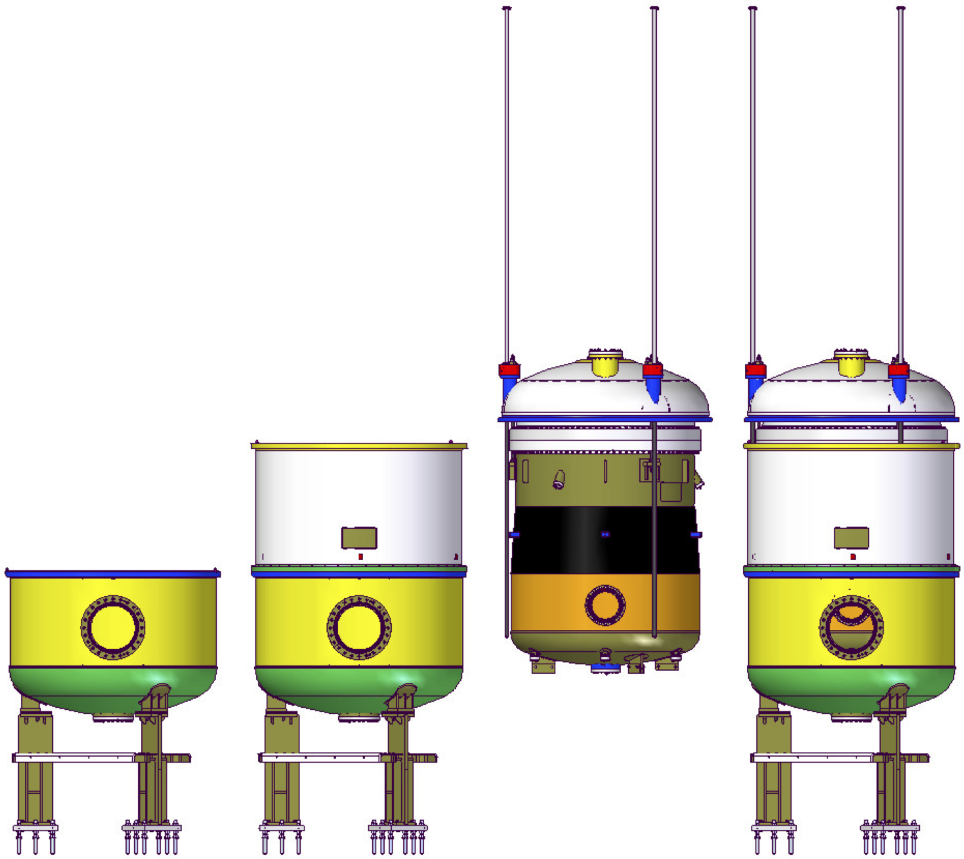

Figure 5.10.1: Major steps of the cryostat assembly underground.

Next in the sequence is the assembly of the ICV into the OCV using a combined lift with the OCV head, tie bar assemblies and ICV. The OCV head and tie bars will have been assembled prior to the start of this procedure, a convenient supporting frame or gantry will be required to set up this lifting operation. Prior to the tie bars being used they must have been assembled and tested using the test equipment. With the ICV in a position accessible for the crane the OCV head complete with tie bars will be lifted over the ICV and the tie bars aligned with the three access holes in the ICV top head flange. Orientation is important as the HV ports of both vessels have to align with adjustment of the tie bars. There is a supporting CS leg at the 0 degree position and a tie bar assembly aligned with this. The HV ports are at 90° to this position. Lower the head and tie bars through the access holes, make sure the top M16 nut and washer is in place before carrying this out. When the tie bar is through its support on the upper part of the ICV assemble the lower M16 nut and washer ensuring that at least twice the diameter is protruding through the nut. Take up the slack with the crane and check dimension of HV port to head flanges and parallelism adjust as necessary. Tighten the M16 nuts and lock tie bars they must not rotate. Lift ICV into OCV with crane, there should be a minimum of three people ensuring that the ICV enters the OCV without hitting the sides, when the head approaches the middle section upper flange place three spacers between the flanges and bring the head into contact with them. Rest the head at this position and check that the HV ports are aligned and that when the spacers are removed the ICV will not hit the bottom of the OCV vessel adjust as necessary. Remove the spacers and lower the OCV head and ICV until the flange engages with the location dowels and mates with the upper flange of the middle section. Secure with 6× M12 bolts and check alignment of HV ports. At this stage the alignment check can be visual if adjustment is needed then use the tie bars but no more than 10mm of adjustment should be used. This assembly procedure at the manufacturers is an assessment of how easy or difficult it is to assemble the vessels and achieve HV port and axis alignment, the foam insulation, MLI, weir piping and bump stops will not be in place but will be for the assembly at SURF.

5.11 Bibliography

[1] D. S. Akerib *et al.* (LUX), "Radio-assay of Titanium samples for the LUX Experiment," (2011), (unpublished), arXiv:1112.1376 [physics.ins-det].

[2] A. Chepurnov, S. Nisi, M. L. di Vacri, and Y. Suvorov, in *LOW RADIOACTIVITY TECHNIQUES 2013 (LRT 2013): Proceedings of the IV International Workshop in Low Radioactivity Technique*, AIP Conf. Proc., Vol. **1549**, edited by L. Miramonti and L. Pandola (2013) pp. 161–164, *The ultra-pure Ti for the low background experiments*, Conference Presentation.

[3] VSMPO-AVISMA, (2015), Parkovaya St. 1, Verkhnaya Salda, Sverdlovsk Region, 624760, Russia.

[4] TIMET, (2015), 224 Valley Creek Blvd. Suite 200, Exton, PA 19341-2300.

[5] Supra Alloys, (2015), 351 Cortez Circle, Camarillo, CA 93012-8638, USA.

[6] "Honeywell Electronic Materials," (2015), 15128 E Euclid Ave, Spokane Valley, WA 99216-1801, USA.

[7] PTG - Performance Titanium Group, (2015), 8400 Miramar Rd Suite 200-248C San Diego, CA 92126-4387, USA.

[8] E. Aprile (XENON1T), in *Proceedings, 10th UCLA Symposium on Sources and Detection of Dark Matter and Dark Energy in the Universe*, Springer Proc. Phys., Vol. **148** (2013) pp. 93–96, *The XENON1T Dark Matter Search Experiment*, Conference Presentation, arXiv:1206.6288 [astro-ph].

[9] X. Cao *et al.* (PandaX), Sci. China Phys. Mech. Astron. **57**, 1476 (2014), arXiv:1405.2882 [physics.ins-det].

[10] K. H. Ackermann *et al.* (GERDA), Eur. Phys. J. **C73**, 2330 (2013), arXiv:1212.4067 [physics.ins-det].

[11] J. J. Gomez-Cadenas (NEXT), *Proceedings, 37th International Conference on High Energy Physics (ICHEP 2014): Valencia, Spain, July 2-9, 2014*, Nucl. Part. Phys. Proc. **273-275**, 1732 (2016), arXiv:1411.2433 [physics.ins-det].

[12] NIRONIT Edelstahlhandel GmbH & Co. KG, (2015), Eckeler Strasse 10, D-21224 Rosengarten, Germany.

[13] W. Maneschg, M. Laubenstein, D. Budjas, W. Hampel, G. Heusser, K. T. Knopfle, B. Schwingenheuer, and H. Simgen (GERDA), Nucl. Instrum. Meth. **A593**, 448 (2008).

[14] V. Álvarez *et al.* (NEXT), J. Instrum. **8**, T01002 (2013), arXiv:1211.3961 [physics.ins-det].

[15] D. S. Akerib *et al.* (LUX), Nucl. Instrum. Meth. **A675**, 63 (2012), arXiv:1111.2074 [physics.data-an].

[16] S. Agostinelli *et al.* (GEANT4), Nucl. Instrum. Meth. **A506**, 250 (2003).

[17] W. B. Wilson, R. T. Perry, W. S. Charlton, and T. A. Parish, Prog. Nucl. Energy **51**, 608 (2009), (SOURCES-4C).

[18] Boiler and Pressure Vessel Committee, *ASME boiler and pressure vessel code, Section VIII, Division 1* (American Society of Mechanical Engineers, Two Park Avenue New York, NY 10016-59905, 2015).

[19] United States Geological Survey, "Seismic Design Maps & Tools," (2015), 12201 Sunrise Valley Dr, Reston, VA 20192-0003.

[20] "ANSYS CFX," (2015), ANSYS, Inc., Southpointe, 2600 ANSYS Drive, Canonsburg, PA 15317-0404; Accessed 12-10-2015.

[21] RUAG, "Cryogenic Insulation Coolcat," (2015), RUAG Holding AG, Stauffacherstrasse 65, 3000 Bern 22 Switzerland.

[22] Technetics Group, (2015), Unit 3 Smitham Bridge Road Hungerford, Berkshire RG17 0QP UK.

[23] Boiler and Pressure Vessel Committee, *ASME boiler and pressure vessel code, Section IX* (American Society of Mechanical Engineers, Two Park Avenue New York, NY 10016-59905, 2015).